# Degradable Vinyl Random Copolymers via Photocontrolled Radical Ring-Opening Cascade Copolymerization

Wenqi Wang,<sup>[a]</sup> Zefeng Zhou,<sup>[a]</sup> Devavrat Sathe,<sup>[b]</sup> Xuanting Tang,<sup>[a]</sup> Stephanie Moran,<sup>[a]</sup> Jing Jin,<sup>[a]</sup> Fredrik Haeffner,<sup>[a]</sup> Junpeng Wang,<sup>[b]</sup> and Jia Niu\*<sup>[a]</sup>

W. Wang, Z. Zhou, X. Tang, S. Moran, Dr. J. Jin, Dr. F. Haeffner, Prof. J. Niu Department of Chemistry

Boston College

Chestnut Hill, Massachusetts 02467, United States

E-mail: jia.niu@bc.edu

[b] D. Sathe, Prof. J. Wang

School of Polymer Science and Polymer Engineering

University of Akron

Akron, Ohio 44325, United States

Supporting information for this article is given via a link at the end of the document.

Abstract: Degradable vinyl polymers by radical ring-opening polymerization are promising solutions to the challenges caused by non-degradable vinyl plastics. However, achieving even distributions of labile functional groups in the backbone of degradable vinyl polymers remains challenging. Herein, we report a photocatalytic approach to degradable vinyl random copolymers via radical ringopening cascade copolymerization (rROCCP). The rROCCP of macrocyclic allylic sulfones and acrylates or acrylamides mediated by visible light at ambient temperature achieved near-unity comonomer reactivity ratios over the entire range of the feed compositions. Experimental and computational evidence revealed an unusual reversible inhibition of chain propagation by in situ generated sulfur dioxide (SO<sub>2</sub>), which was successfully overcome by reducing the solubility of SO<sub>2</sub>. This study provides a powerful approach to degradable vinyl random copolymers with comparable material properties to non-degradable vinyl polymers.

### Introduction

Vinyl polymers have been widely used in an array of applications including packaging, structural materials, synthetic fibers, coating, absorbents, and many others. While the all-carbon backbone makes vinyl polymers highly robust materials, it has also created significant challenges in their degradation, leading to critical environmental issues including plastic accumulation in landfills and the ocean. 1-2 Therefore, significant efforts have been made in recent years to develop innovative synthetic polymers that possess thermal and mechanical properties comparable to the original nondegradable vinyl polymers, but can undergo facile degradation at the end of their life cycle.3-4 Among various approaches to degradable vinyl polymers, radical ring-opening polymerization (rROP) is of great interest. Attractive features of rROP include its ability to incorporate labile functional groups (e.g., esters, thioesters, disulfide, etc.) into the polymer main chain<sup>5-7</sup> and the ability to interface with reversible deactivation radical polymerization (RDRP) techniques for the synthesis of polymers with complex and defined macromolecular architectures.8

Since the advent of rROP, various cyclic monomers have been successfully developed for the synthesis of degradable vinyl (co)polymers.<sup>6</sup> As a representative class of rROP monomer, cyclic ketene acetals (CKAs) have been extensively investigated since the 1980s.9 Despite recent progress made by Dove, 10-14 Nicolas, 15-20 and Sumerlin, 21-22 unfavorable reactivity ratios in the copolymerization of CKAs with other vinyl monomers often led to gradient or tapered compositions of the resultant copolymer.<sup>23</sup> The gradient composition in turn resulted in highly dispersed degradation products and large non-degradable fragments, as part of the copolymer lacked main-chain degradable units. Although new cyclic monomer classes including macrocyclic allylic sulfides (MASs)24-27 and dibenzo[c,e]oxepane-5-thiones (DOTs)<sup>28-30</sup> (Figure 1A) have demonstrated promising properties, ideal random copolymers of these cyclic monomers with acrylates or acrylamides, which require both comonomer reactivity ratios to equal one in copolymerization, remain challenging. In 2018, we reported an approach to thermally initiated radical ring-opening cascade polymerization of allylic sulfone macrocyclic monomers.31 The radical cascade reaction of the macrocyclic allylic sulfone could extrude sulfur dioxide (SO<sub>2</sub>) and generate a secondary alkyl radical capable of controlled chain propagation.<sup>32</sup> However, the macrocyclic allylic sulfone exhibited a significantly faster rate of incorporation than acrylates in the thermally initiated copolymerization, resulting in unfavorable comonomer reactivity ratios. Therefore, it is essential to develop a method that provides access to ideal random copolymers with tunable compositions and evenly distributed main-chain functional groups.

Previous studies have suggested that temperature has a strong influence on the reactivity ratios during the radical copolymerization of cyclic and acyclic vinyl comonomers. 6,33 We reasoned that performing the copolymerization at lower temperatures would provide a key opportunity to modulate the reactivity ratios of vinyl comonomers. Therefore, we turned our attention to light-mediated polymerization techniques, as recent works have demonstrated that they are versatile tools to mediate controlled polymerization following radical, 34-42 cationic, 43-47 and metathesis pathways 48-50 at ambient temperature (Figure 1B). 51 In particular, we envisioned that the photoinduced electron/energy transfer-reversible addition/fragmentation chain transfer (PET-RAFT) polymerization developed by Boyer and coworkers 52-56 could be employed to mediate the radical ring-opening cascade copolymerization (rROCCP) 57-58 of the macrocyclic allylic sulfone

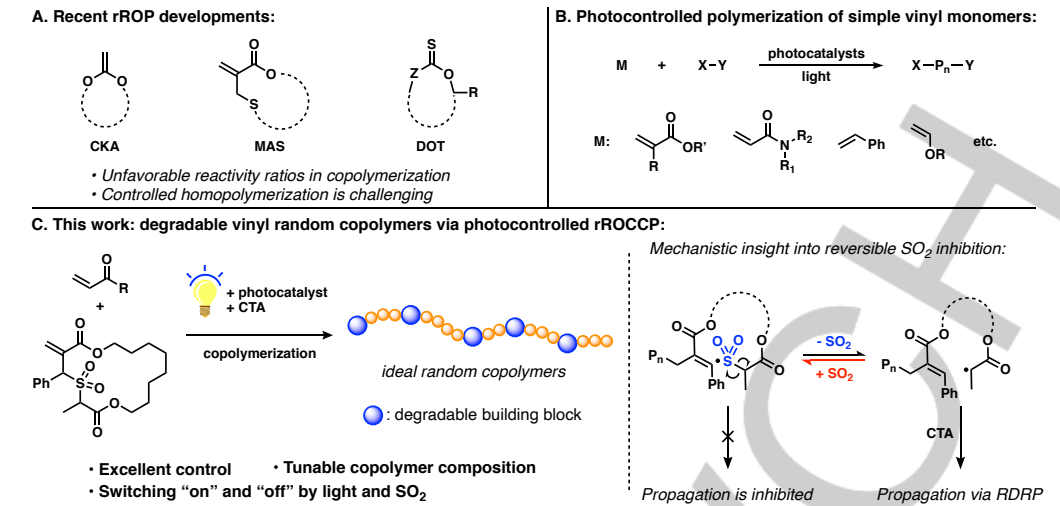


Figure 1. Degradable vinyl random copolymers via photocontrolled radical ring-opening cascade copolymerization (rROCCP).

with acrylates or acrylamides (Figure 1C). Unlike the polymerization that is thermally initiated by azobisisobutyronitrile (AIBN), which requires high temperatures (80-100 °C) to maintain a sufficiently high rate of propagation, PET-RAFT can be performed at mild temperatures, thereby enabling favorable comonomer reactivity ratios in copolymerization. <sup>59</sup> To the best of our knowledge, photocontrolled rROCCP represents the first general approach to nearly ideal random copolymers of cyclic and acrylic monomers over the entire range of the comonomer feed compositions.

#### **Results and Discussion**

Our investigation began by screening various wellestablished photocatalysts to mediate the photocontrolled homopolymerization of allylic sulfone macrocyclic monomer 1 under visible light irradiation (Table S1).52-56 We screened an array of photocatalysts, including fac-[Ir(ppy)3], Ru(bpy)3Cl2, ZnTPP, and Eosin Y. We identified fac-[Ir(ppy)3] as a promising photocatalyst for the reaction due to the excellent control over the polymerization when combined with CTA1. At a monomer/CTA ratio of 50:1, our initial attempt of the polymerization of macrocyclic allylic sulfone 1 mediated by fac-[lr(ppy)3] and CTA1 under 450 nm light irradiation yielded P-1 with  $M_n^{(SEC)}$  of 9.8 kg/mol and Đ of 1.11 (Table S2). Further examination of the reaction conditions revealed that the optimal polymerization was achieved when the monomer concentration was 0.2 M in DMF and the catalyst loading was 200 ppm (Table S3-S5). Polymerization of 1 at other monomer/CTA ratios of 25:1, 100:1, and 200:1 successfully yielded polymers with predictable  $M_n$  and low  $\mathcal{D}$ , demonstrating excellent control over the polymerization (Table S6). Similarly, macrocyclic allylic sulfone 2, which contains a smaller ring, was also polymerized with good control under the same conditions (Table S7). It is noteworthy that no ring-retaining propagation of both allylic sulfone macrocyclic monomers 1 and 2 has been observed.

Following the exploration of the reaction conditions, we examined the living characteristics of the polymerization. First, the kinetic analysis revealed that the polymerization of 1 deviated from first-order kinetics in the late stage (Figure S1). This observation was consistent with our previous results when the

cascade polymerization of the macrocyclic allylic sulfone was thermally initiated. 31,60 Despite the kinetic anomaly, the polymerization of 1 still exhibited a linear increase of  $M_n$  with respect to the monomer conversion and retained low D throughout the reaction, suggesting that control over the polymerization was well maintained even after the rate decreased in the late stage (Figure 2A). <sup>1</sup>H-NMR analysis of **P-1-6k** (M<sub>n</sub>(SEC) = 6.4 kg/mol,  $\theta$  = 1.07) confirmed the fidelity of the chain end groups (2.46 and 1.21 ppm for  $\alpha$ -chain end and 4.81 and 3.36 ppm for w-chain end, Figure S2), an important indicator of controlled polymerization. Besides, the discrete oligomers of P-1-**5k**  $(M_n^{(SEC)} = 5.5 \text{ kg/mol}, D = 1.10)$  observed by matrix-assisted laser desorption/ionization time-of-flight (MALDI-TOF) mass spectrometry showed masses consistent with the predicted values of these oligomers with intact chain ends (Figure 2B). Furthermore, chain extension of the macroinitiator P-2-4k (M<sub>n</sub>(SEC) = 3.9 kg/mol,  $\theta$  = 1.16) by 1 exhibited a clear shift to the higher molecular weight region on size-exclusion chromatogram (SEC), suggesting the formation of a diblock copolymer P-2-b-P-1  $(M_n^{(SEC)} = 13.0 \text{ kg/mol}, D = 1.20, Figure 2C)$ . Finally, the reaction exhibited excellent temporal control: chain propagation completely halted when the light was switched "off"; polymerization resumed efficiently after the light was switched back "on" (Figure 2D). Taken together, these results unambiguously supported that the PET-RAFT polymerization of the macrocyclic allylic sulfone maintained an excellent control throughout the reaction despite the deviation from first-order kinetics at the late stage.

Building upon the results of the photocontrolled homopolymerization of macrocyclic allylic sulfones, we then investigated the copolymerization of 1 and various acrylates or acrylamides (denoted hereafter as comonomer B). First, 1 was copolymerized with methyl acrylate (MA) at a feed composition of  $f_1^0 = 0.05$ , where  $f_1^0$  is the molar fraction of 1 in the initial comonomer mixture, yielding copolymer P-1-co-MA with  $M_n^{(SEC)}$  of 44.0 kg/mol and D of 1.28 (Table 1, entry 1). The propagation of both comonomers demonstrated first-order kinetics throughout the copolymerization (Figure 3A). The molecular weight also increased linearly with respect to the overall monomer conversion, which is defined by Eq 1:

$$conv. = 1 - \frac{[1(t)] + [B(t)]}{[1(0)] + [B(0)]} \tag{1}$$

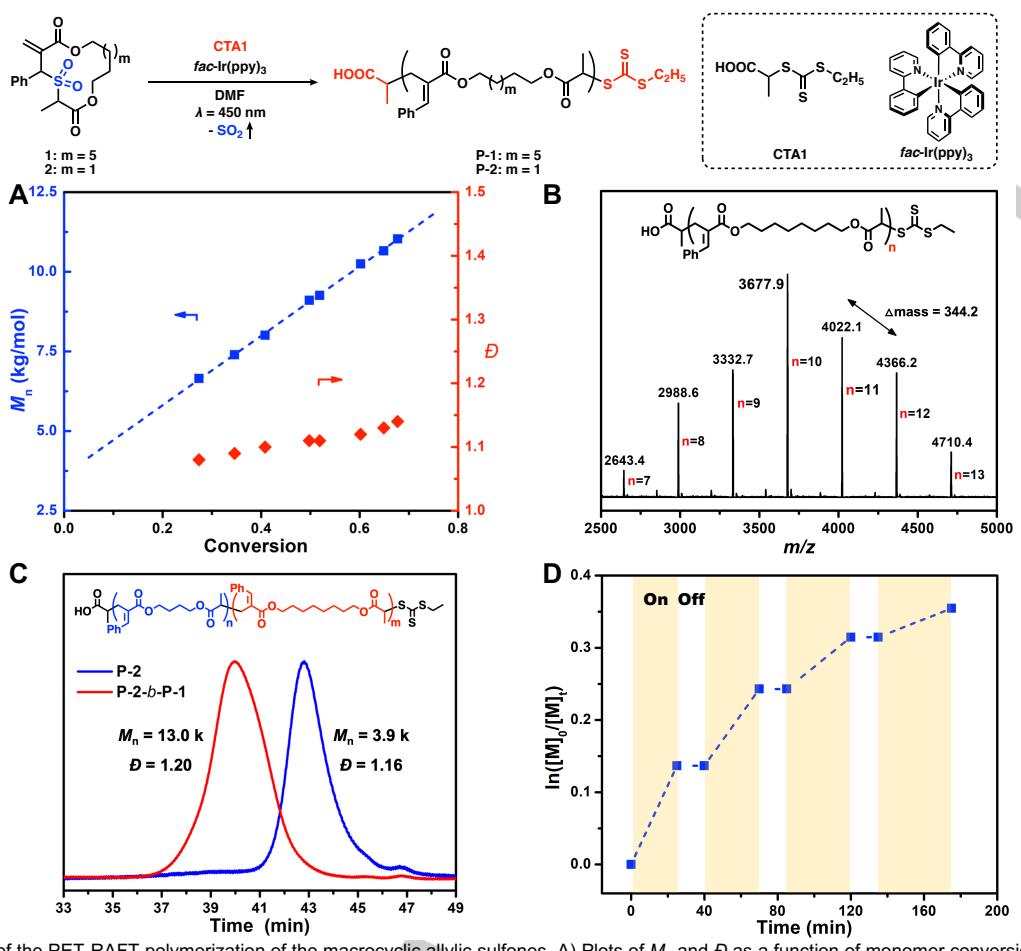


Figure 2. Analysis of the PET-RAFT polymerization of the macrocyclic allylic sulfones. A) Plots of  $M_n$  and D as a function of monomer conversion. B) MALDI-TOF analysis of **P-1-5k**. The spacing between these discrete oligomers was consistent with the expected mass of the repeating unit (344 g/mol). Each peak corresponds to a discrete oligomer that consists of the α- and ω-chain end, the number of repeating units multiplied by its molar mass, and a sodium cation. C) SEC analysis of block copolymer **P-2-b-P-1**. D)  $\ln([M]_0/[M]_1)$  vs. reaction time with intermittent light exposure.

where [1(t)] and [B(t)] are the respective instantaneous concentrations of 1 and comonomer B at time t, and [1(0)] and [B(0)] are the respective initial concentrations of 1 and comonomer B (Figure 3B). Importantly, the instantaneous molar fraction of 1 incorporated in the copolymer (denoted hereafter as  $F_1$ ) remained identical to  $f_1^0$  throughout the copolymerization (Figure S3). Correspondingly, the final copolymer composition,  $F_1^{(end)}$ , when the reaction reached the end point, was also identical to  $f_1^0$  (Table 1, entry 1). These results suggested that the reactivities of the two comonomers are highly similar in chain propagation. To determine the reactivity ratios of the copolymerization, the compositional data of 1 and B throughout the copolymerization was fitted to the Beckingham–Sanoja–Lynd (BSL) integrated model reported by Lynd et al.  $^{61}$ 

$$conv. = 1 - f_1^0 \left[ \frac{1(t)}{1(0)} \right] - (1 - f_1^0) \left[ \frac{1(t)}{1(0)} \right]^{r_B}$$
 (2)

$$conv. = 1 - f_1^0 \left[ \frac{B(t)}{B(0)} \right]^{r_1} - (1 - f_1^0) \left[ \frac{B(t)}{B(0)} \right]$$
 (3)

where  $r_1$  and  $r_B$  are the reactivity ratios of **1** and comonomer B. It is noteworthy that although the BSL model is derived for ideal copolymerization where the product of the comonomer reactivity ratios equals unity, such as ionic or metal-catalyzed copolymerization systems, we reasoned that the

copolymerization of the macrocyclic allylic sulfone and acrylic monomers is a close approximation of ideal copolymerization, because the allylic sulfone motif was designed such that the propagating secondary alkyl radical formed after the radical cascade process is structurally similar to the propagating radical polyacrylates.62 Independent fitting of the polymer compositional data to Eq 2 and Eq 3 supported this rationale, as the derived reactivity ratios of the comonomers were  $r_1$  = 1.07±0.03 and  $r_B$  = 0.94±0.02, with  $r_1 \times r_B$  = 1.01±0.05 (Figure 3C). These results suggested that the copolymerization reaction is indeed highly analogous to an ideal copolymerization and that the copolymer generated from the reaction is very close to an ideal random copolymer. The reactivity ratios of 1 and MA in the entire range of the monomer feed compositions ( $f_1^0 = 0-1$ ) remained close to unity (Table 1, entries 1-6 & Figure 3D & Figure S4-13). Furthermore, the copolymerization of 1 with other acrylic comonomers, including tert-butyl acrylate (tBA), benzyl acrylate (BnA), N,N-dimethylacrylamide (DMA), N,N-diethylacrylamide (DEA), and N-Acryloylmorpholine (NAM), at  $f_1^0 = 0.09$  all exhibited excellent control over the polymerization and near-unity reactivity ratios, suggesting that this method is generally applicable to a wide range of acrylates and acrylamides (Table 1, entries 7-11 & Figure S14-23). As acrylates and N,Ndialkylacrylamides have been shown to exhibit similar reactivities in radical copolymerization, 63-64 our results further indicate that

Table 1. Photocontrolled rROCCP of 1 and various acrylates or acrylamides.

Entry <sup>a</sup>	В	$f_1^0$	$r_1{}^b$	$r_B^{\ b}$	Conv.c	M <sub>n</sub> (SEC) (kg/mol) <sup>d</sup>	Đ <sup>d</sup>	$F_{1}^{(end)_{\mathcal{C}}}$	Degraded  M <sub>n</sub> (SEC) (kg/mol) d	Degraded Đ <sup>d</sup>
1	MA	0.05	1.07±0.03	0.94±0.02	88%	44.0	1.28	0.05	2.8	1.58
2	MA	0.09	1.05±0.03	0.95±0.02	82%	21.7	1.27	0.10	1.3	1.33
3	MA	0.17	1.04±0.03	0.96±0.02	76%	14.8	1.15	0.17	0.7	1.30
4	MA	0.50	1.06±0.03	0.94±0.03	70%	9.3	1.12	0.51	0.6	1.12
5	MA	0.67	1.04±0.03	0.96±0.03	75%	7.7	1.18	0.68	0.5	1.07
6	MA	0.80	1.04±0.06	0.97±0.07	61%	6.8	1.17	0.80	0.5	1.06
7	<i>t</i> BA	0.09	1.04±0.04	0.96±0.03	85%	39.0	1.29	0.09	2.6	1.34
8	BnA	0.09	0.84±0.03	1.19±0.04	89%	22.1	1.38	0.08	2.9	1.35
9	DMA	0.09	1.03±0.03	0.97±0.03	75%	16.1	1.21	0.09	1.8	1.42
10	DEA	0.09	0.89±0.06	1.16±0.08	79%	20.1	1.14	0.07	2.2	1.38
11	NAM	0.09	0.94±0.05	1.07±0.06	82%	20.9	1.34	0.09	2.8	1.32

<sup>a</sup>Experimental conditions: 18 W blue LED light ( $\Lambda_{max}$  = 450 nm), 25 °C under argon in a sealed vial for 8 h; light intensity at the reaction vial = 34 mW/cm<sup>2</sup>. <sup>b</sup> The reactivity ratios were obtained by fitting the comonomer conversion and composition of copolymers to the BSL integrated model. The mean and 95% confidence interval of the reactivity ratios were calculated based on five to seven independent fitting results. <sup>c</sup>Monomer conversion and  $F_1^{(end)}$  were determined by <sup>1</sup>H NMR spectroscopy. <sup>d</sup>M<sub>n</sub> and D were determined by SEC analysis calibrated to polystyrene standards.

the macrocyclic allylic sulfone, which is designed to resemble acrylates in radical propagation, also possesses a similar reactivity to these two monomer classes.

To investigate how the degradability was influenced by the composition and distribution of the degradable building blocks in the copolymers, the copolymers were treated with sodium methoxide to cleave the main-chain esters. SEC analysis of the P-(1-co-MA) prepared degradation of copolymer photocontrolled rROCCP ( $F_1^{(end)} = 0.10$ ,  $M_n^{(SEC)} = 19.2$  kg/mol, and  $\theta$  = 1.27) exhibited a dramatic molecular weight reduction, resulting in oligomers with  $M_n^{(SEC)}$  of 1.3 kg/mol and  $\theta$  of 1.33 (Table 2, entry 2 & Figure 4A). In contrast, degradation of the copolymer with a similar overall composition ( $F_1^{(end)} = 0.08$ ,  $M_n^{(SEC)}$  = 16.4 kg/mol, and  $\theta$  =1.52) generated by thermallyinitiated copolymerization produced fragments with higher  $M_n$  and  $D(M_n^{(SEC)} = 7.3 \text{ kg/mol}, D = 1.98)$  (Figure 4A). Furthermore, the degradation of copolymers with different comonomer compositions generated by photocontrolled rROCCP consistently produced fragments with low  $M_n$  and narrow molecular weight distributions (Table 1). These results indicated that while the

thermally initiated copolymerization yielded a gradient copolymer that could only be partially degraded, copolymers generated by photocontrolled rROCCP possessed even and tunable distributions of the main-chain degradable functionalities that could be degraded efficiently into low molecular weight fragments.

The thermal properties of the copolymers were evaluated by thermogravimetry (TGA) and differential scanning calorimetry (DSC) analyses. **P-(1-co-MA)** with main-chain degradable functionalities at different copolymer compositions exhibited a thermal stability comparable to that of poly(methyl acrylate) (PMA) with a 5% weight loss decomposition temperature ( $T_d$ ) between 363-368 °C (Figure 4B). Furthermore, the glass transition temperature ( $T_g$ ) of **P-(1-co-MA)** can be fine-tuned by the initial comonomer feed composition in the copolymerization, highlighting the potential utility of this method in generating degradable vinyl polymers with tailor-made material properties (Figure 4C). The thermomechanical properties of **P-(1-co-MA)** ( $F_1^{(end)} = 0.05$ ) and PMA were further studied using temperature sweep measurements with a parallel plate rheometer. The  $T_g$ s measured from the storage moduli (G') for **P-(1-co-MA)** and PMA

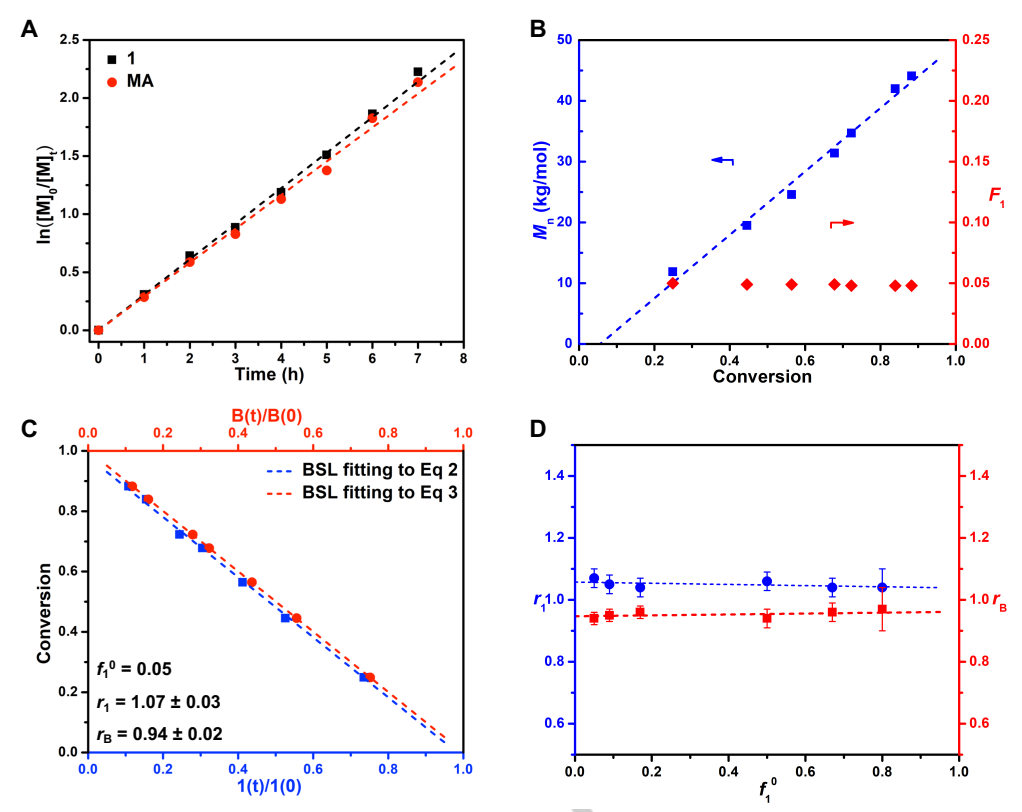


Figure 3. Photocontrolled rROCCP of the macrocyclic allylic sulfone and various acrylates and acrylamides generates nearly ideal random copolymers. A) Kinetic plots of  $\ln([M]_0/[M]_1)$  versus reaction time of both comonomers. B) Plots of  $M_n$  and incorporation of 1 ( $F_1$ ) as a function of total conversion. C) The plot of total conversion with respect to [1(t)]/[1(0)] or [B(t)]/[B(0)] is fitted to Eq 2 and Eq 3 of the BSL model independently to derive the reactivity ratios. D) The reactivity ratios of 1 and MA in photocontrolled rROCCP remained close to unity in a broad range of monomer feed compositions. The error bars indicate the 95% confidence interval of the reactivity ratios.

were 4.6 °C and 13 °C (Figure 4D), respectively, which agree well with the DSC analyses. Furthermore, the onset of the terminal region for **P-(1-co-MA)** was 31.5 °C, while the value for PMA was 41.2 °C. Similar to the effect on  $T_g$ , incorporation of 5% of 1 only resulted in minimal impacts on the mechanical properties of the polymer; the G at the onset of the rubbery plateau was ~0.4 MPa for PMA and 0.3 MPa for **P-(1-co-MA)**. Compared to PMA, the slightly larger  $\tan(\delta)$  peaks for **P-(1-co-MA)** during the glass transition and during the transition to the terminal region indicate slightly higher viscous responses to deformation.

while PET-RAFT Our studies have shown that homopolymerization and copolymerization (Figure S1 & S24-32) involving macrocyclic allylic sulfones deviated from first-order kinetics, the polymerization remained well-controlled. This phenomenon was in stark contrast to traditional controlled polymerization in which the deviation from first-order kinetics is usually a sign of loss of control, suggesting an unusual kinetic behavior that warranted further investigation. Furthermore, the near-unity reactivity ratios of the comonomers during photocontrolled rROCCP at lower temperatures also differ from some conventional radical copolymerization systems, in which comonomer reactivity ratios move further away from unity when temperature decreases. 33 We suspected that the in situ generated SO<sub>2</sub> during the radical cascade process affected the reaction kinetics and comonomer reactivities in the copolymerization (Figure 5A). 65-67

To investigate this hypothesis, Density Functional Theory (DFT) calculations were carried out using the M06-2X/6-311++G(d,p)//B3LYP/6-31G(d) method in conjunction with the Solvation Model based on Density (SMD) simulating the effect

from DMF to compute a plausible potential energy surface of the cascade process in the polymerization of macrocyclic allylic sulfones (Figure 5B).  $^{68}$  Our calculations showed that the lphascission/SO<sub>2</sub> extrusion step (G<sub>2</sub> to G<sub>3</sub>) has a low energy barrier of 5.9 kcal/mol, and that the transformation is exergonic by 2.8 kcal/mol. The low activation energy and relatively small change in Gibbs free energy indicate that this step is likely reversible. The DFT calculations also suggest that G<sub>3</sub>, with the lowest energy in the whole cascade process, exists at a high enough concentration during steady-state conditions, making it a plausible intermediate for chain propagation (Figure S33). Compared to chain propagation (G<sub>3</sub>-TS<sub>4</sub>-G<sub>4</sub>, with an energy barrier of 20.7 kcal/mol), two alternative reaction pathways of G3 with lower energy barriers are the reversible addition by the CTA (G3-TS5-G5, with an energy barrier of 12.0 kcal/mol) or SO<sub>2</sub> (G<sub>3</sub>-TS<sub>3</sub>-G<sub>2</sub>, with an energy barrier of 8.7 kcal/mol). While the former serves as the reversible deactivation of the chain propagation to achieve controlled polymerization, the latter is a reverse reaction of the  $\alpha$ scission/SO<sub>2</sub> extrusion step and regenerates the sulfonyl radical G2. Because of a high energy barrier of 19.7 kcal/mol and being endergonic by 9.8 kcal/mol, chain propagation of G2 by the monomer (G2-TS6-G6) is prohibited thermodynamically and kinetically. These results indicate that excess SO2 in the reaction could indeed recombine with the propagating alkyl radical to regenerate the sulfonyl radical and inhibit chain propagation.

To provide further evidence of the presence and accumulation of the sulfonyl radicals over the course of the reaction, we employed electron paramagnetic resonance (EPR) to monitor the evolution of radical species in the reaction *in situ* (Figure 5C). In the early stage (initial two hours) of the reaction,

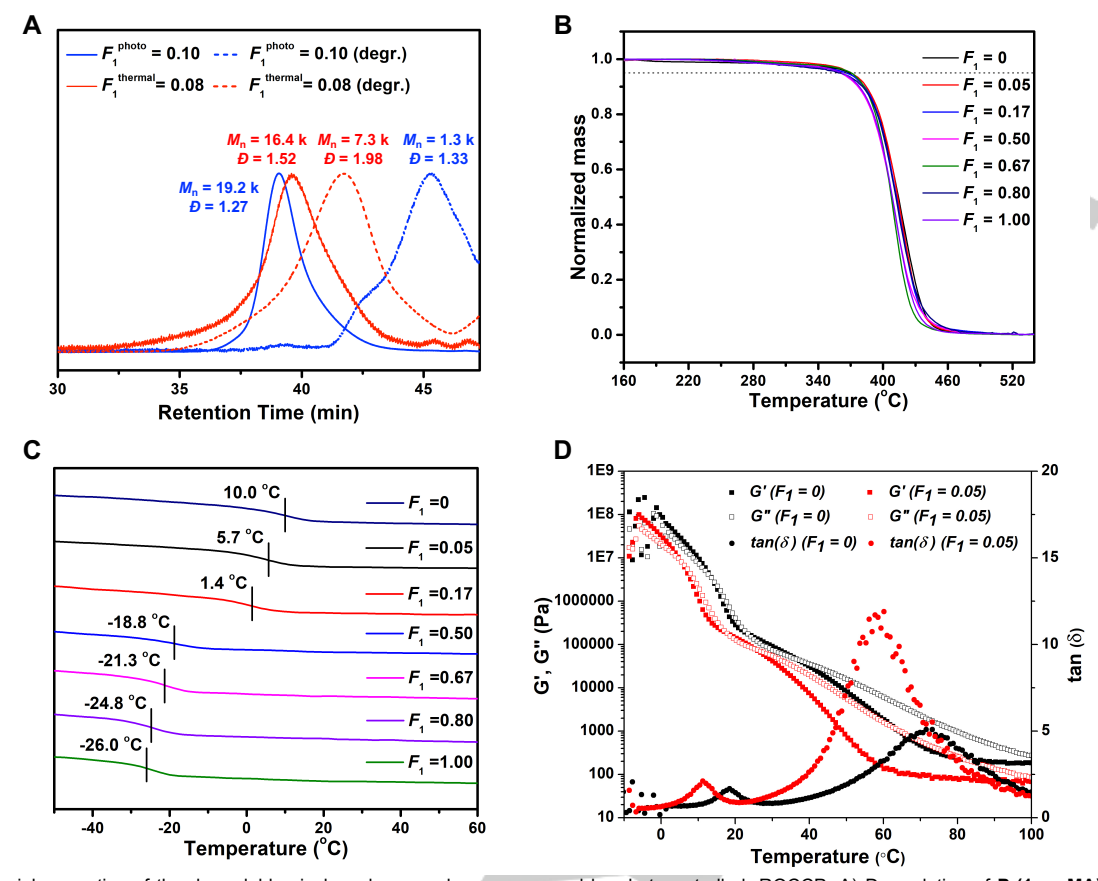


Figure 4. Material properties of the degradable vinyl random copolymers prepared by photocontrolled rROCCP. A) Degradation of **P-(1-co-MA)** generated by photocontrolled copolymerization ( $I_1^{(end)} = 0.10$ ) and thermally initiated radical copolymerization ( $I_1^{(end)} = 0.08$ ) respectively. B) The  $T_d$  of the copolymers **P-(1-co-MA)** with different compositions demonstrated a similar thermal stability with PMA. C) The  $T_g$  of the copolymers **P-(1-co-MA)** could be fine-tuned by the initial comonomer feed composition. D) The storage moduli, loss moduli, and  $tan(\delta)$  for PMA and **P-(1-co-MA)** ( $I_1^{(end)} = 0.05$ ) obtained from rheological measurements.

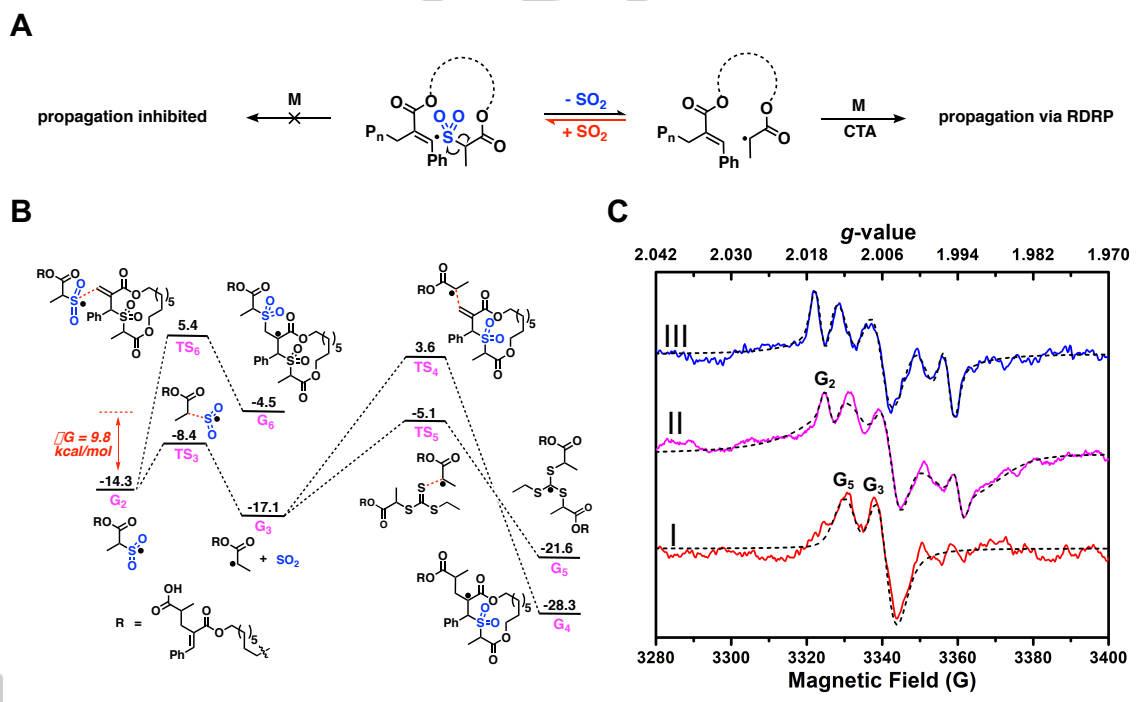
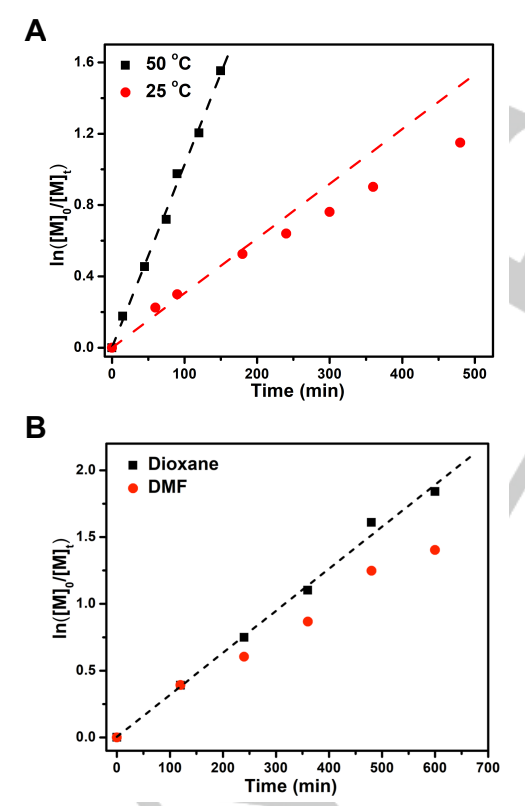


Figure 5. Mechanistic investigation of the cascade process of the polymerization of the macrocyclic allylic sulfone. A) SO<sub>2</sub> is hypothesized to inhibit chain propagation by recombining with the propagating radical. M denotes monomers. B) DFT calculations. C) EPR studies of the polymerization of the macrocyclic allylic sulfones. The experimental results are shown as solid lines. The simulated EPR spectra based on the hypothesized composition of the reaction mixture at different stages of the reaction are shown as dotted lines. The experimental EPR spectra are well aligned with the simulated ones. Spectrum I: Early stage of polymerization (first two hours). Spectrum III: Late stage of polymerization (after five hours). Spectrum III: Injection of exogenous SO<sub>2</sub> at the early stage of polymerization.

the EPR spectrum only consisted of signals corresponding to the alkyl radical  $G_3$  ( $g_0 = 2.004$ ) and the degenerative intermediate  $G_5$  $(g_0 = 2.009)$  (Spectrum I, Figure 5C). The g-values of the peaks and patterns of the spectrum are both consistent with the radical species generated in the radical polymerization of MA. The EPR spectrum gradually evolved as the polymerization proceeded. In the late stage (after five hours) of the reaction, a new peak with a g-value of 2.014 appeared in the EPR spectrum (Spectrum II, Figure 5C), which is consistent with the g-value of the sulfonyl radical G<sub>2</sub> reported in literature. <sup>69</sup> Furthermore, the simulated EPR spectra (dotted lines) based on the absence and presence of the sulfonyl radical in the reaction perfectly fit the experimental data as shown in Spectrum I and II, respectively, confirming the proposed assignments. Notably, Spectrum II is also consistent with Spectrum III obtained after the exogenous SO2 gas was introduced to the system at the early stage of the reaction (Figure 5C). Collectively, the DFT calculations and EPR analyses are consistent with the observed kinetic results, confirming that G2,  $G_3$ , and  $G_5$  (Figure 5B & 5C) are long-lived radical intermediates in the polymerization of the macrocyclic allylic sulfone, and that the concentration of SO<sub>2</sub> could have a significant effect on the direction of the reaction. The inhibition of the chain propagation by SO<sub>2</sub> also explains the favorable comonomer reactivity ratios in photocontrolled rROCCP at lower temperatures, as SO2 likely retards the rate of incorporation of the macrocyclic allylic sulfone more than that of acrylates/acrylamides when the temperature decreases.



**Figure 6.** Inhibition of the propagation by SO<sub>2</sub> is reversible. A) Pseudo-first-order kinetics was achieved in the PET-RAFT homopolymerization of **1** by elevating the temperature to 50 °C plus argon sparging. B) Photocontrolled rROCCP of **1** and BnA at  $f_1^0$  = 0.09 in dioxane remained pseudo-first-order throughout the reaction.

Based on the DFT calculations, we reason that the propagation inhibition by the  $in\ situ$  generated SO<sub>2</sub> may be reversible, given the low energy barrier of the process. This

reversibility implies that the extrusion of SO2 and the formation of the alkyl radical are favored at low SO2 concentrations, whereas the recombination of SO<sub>2</sub> and the formation of the sulfonyl radical are favored at high SO<sub>2</sub> concentrations. Therefore, the propagation inhibition could be alleviated by removing SO2 from the reaction. Indeed, we found that sparging the reaction mixture with argon steadily increased the rate of PET-RAFT homopolymerization of 1 in the late stage of the reaction at 25 °C (Figure S34). In fact, both the SO2 inhibition and reactivation of the chain propagation by argon sparging were reversible and the polymerization could be switched "on"/"off" by alternating the exogenous SO2 and argon introduced into the reaction vessel (Figure S35-S36). Similarly, the propagation inhibition was also alleviated in the copolymerization of 1 and BnA ( $f_1^0 = 0.09$ ) by argon sparging at 25 °C (Figure S37). Additionally, increasing the reaction temperature to 50 °C was also found to improve the rate of PET-RAFT homopolymerization of 1 in the late stage (Figure \$38-\$39). Combining the argon sparging and the temperature elevation to 50 °C further improved the reaction kinetics of PET-RAFT homopolymerization of 1, allowing it to remain pseudo-firstorder throughout the reaction (Figure 6A). The rate of the copolymerization of 1 and MA was also improved when the reaction temperature was elevated to 50 °C (Figure S40), but a modest deviation of the comonomer reactivity ratios from unity was observed (Figure S41). We reasoned that an alternative strategy to reduce the propagation inhibition by SO2 was to switch the solvent from DMF to dioxane, in which SO2 has lower solubility (Figure S42). Encouragingly, we found that the kinetics of copolymerization of 1 and BnA at 25 °C remained pseudo-firstorder throughout the reaction when dioxane was used as the solvent (Figure 6B).

## Conclusion

A general approach to the degradable vinyl random copolymers with tunable main-chain compositions photocontrolled radical ring-opening cascade copolymerization (rROCCP) is presented in this article. Compared to existing rROP systems, photocontrolled rROCCP enabled the synthesis of degradable vinyl random copolymers with evenly distributed, tunable composition of main-chain labile groups at ambient temperature. These copolymers demonstrated readily tunable  $T_{\rm g}$ s based on the composition, and possess thermal and mechanical properties comparable to the corresponding nondegradable homopolymers when the composition of the main-chain labile groups was kept low (e.g.,  $F_1^{(end)} = 0.05$ ). Computational and EPR analyses revealed that the reversible inhibition of the chain propagation by the in situ generated SO2 caused an unusual kinetic behavior that showed a deviation from first-order kinetics in the late stage of the reaction. Removal of SO2 was found to reverse the inhibition of the chain propagation and improve the reaction kinetics in both the homopolymerization and the copolymerization involving the macrocyclic allylic sulfone. Taken together, excellent control and favorable comonomer reactivity ratios make photocontrolled rROCCP a powerful strategy for the preparation of degradable vinyl random copolymers with tunable main-chain compositions for a wide range of applications. In addition, the mechanistic insights into the reversible inhibition of chain propagation by SO2 shed light on using chemical cues to control radical chain-growth cascade polymerization systems.

#### Acknowledgements

We thank Marek Domin, Jiangwei Liu, Matthew Thompson, Miao Qi, Junfeng Zhou, Gavin Giardino, Jingsong Yuan, Lianqian Wu, Cangjie Yang, Hanchu Huang, and Jeff Byers for characterization assistance and helpful discussions. The research is primarily supported by a CAREER award from the National Science Foundation (CHE-1944512) to J.N. Financial support is also provided by the Arnold and Mabel Beckman Foundation through a Beckman Young Investigator Award to J.N. and an American Chemical Society Petroleum Research Fund Doctoral New Investigator Award (60747DNI7) to J.N.

#### **Conflict of Interest**

A provisional patent based on this work has been filed.

**Keywords:** photocontrolled polymerization • cascade polymerization • degradable polymer • random copolymer • reaction mechanism

- [1] R. Geyer, J. R. Jambeck, K. L. Law, Sci. Adv. 2017, 3, e1700782.
- [2] M. E. Seeley, B. Song, R. Passie, R. C. Hale, Nat. Commun. 2020, 11, 2372.
- [3] V. Delplace, J. Nicolas, Nat. Chem. 2015, 7, 771-784.
- [4] M. Mohadjer Beromi, C. R. Kennedy, J. M. Younker, A. E. Carpenter, S. J. Mattler, J. A. Throckmorton, P. J. Chirik, Nat. Chem. 2021,13, 156-162.
- [5] W. J. Bailey, *Polym. J.* **1985**, *17*, 85-95.
- [6] A. Tardy, J. Nicolas, D. Gigmes, C. Lefay, Y. Guillaneuf, *Chem. Rev.* 2017, 117, 1319-1406.
- [7] T. Pesenti, J. Nicolas, ACS Macro Lett. 2020, 9, 1812-1835.
- [8] N. Corrigan, K. Jung, G. Moad, C. J. Hawker, K. Matyjaszewski, C. Boyer, Prog. Polym. Sci. 2020, 111, 101311.
- [9] W. J. Bailey, Z. Ni, S.-R. Wu, J. Polym. Sci., Polym. Chem. Ed. 1982, 20, 3021-3030.
- [10] G. G. Hedir, C. A. Bell, N. S. leong, E. Chapman, I. R. Collins, R. K. O'Reilly, A. P. Dove, *Macromolecules* 2014, 47, 2847-2852.
- [11] G. G. Hedir, C. A. Bell, R. K. O'Reilly, A. P. Dove, *Biomacromolecules* 2015, 16, 2049-2058.
- [12] C. A. Bell, G. G. Hedir, R. K. O'Reilly, A. P. Dove, *Polym. Chem.* 2015, 6. 7447-7454.
- [13] G. G. Hedir, M. C. Arno, M. Langlais, J. T. Husband, R. K. O'Reilly, A. P. Dove, *Angew. Chem. Int. Ed.* **2017**, *56*, 9178-9182.
- [14] G. Hedir, C. Stubbs, P. Aston, A. P. Dove, M. I. Gibson, ACS Macro Lett. 2017. 6. 1404-1408.
- [15] V. Delplace, E. Guegain, S. Harrisson, D. Gigmes, Y. Guillaneuf, J. Nicolas, Chem. Commun. 2015, 51, 12847-12850.
- [16] J. Tran, E. Guegain, N. Ibrahim, S. Harrisson, J. Nicolas, *Polym. Chem.* 2016, 7, 4427-4435.
- [17] A. Tardy, J.-C. Honore, J. Tran, D. Siri, V. Delplace, I. Bataille, D. Letourneur, J. Perrier, C. Nicoletti, M. Maresca, C. Lefay, D. Gigmes, J. Nicolas, Y. Guillaneuf, *Angew. Chem. Int. Ed.* 2017, 56, 16515-16520.
- [18] E. Guegain, J.-P. Michel, T. Boissenot, J. Nicolas, Macromolecules 2018, 51, 724-736.
- [19] E. Guegain, J. Tran, Q. Deguettes, J. Nicolas, Chem. Sci. 2018, 9, 8291-8306.
- [20] E. Guegain, C. Zhu, E. Giovanardi, J. Nicolas, *Macromolecules* 2019, 52, 3612-3624.
- [21] M. R. Hill, E. Guegain, J. Tran, C. A. Figg, A. C. Turner, J. Nicolas, B. S. Sumerlin, ACS Macro Lett. 2017, 6, 1071-1077.
- [22] M. R. Hill, T. Kubo, S. L. Goodrich, C. A. Figg, B. S. Sumerlin, Macromolecules 2018, 51, 5079-5084.

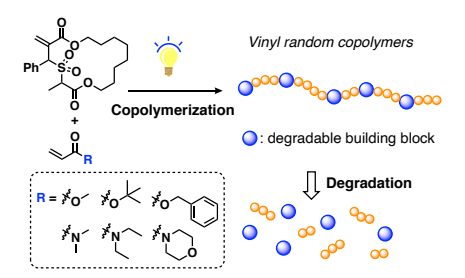
- [23] A. Tardy, N. Gil, C. M. Plummer, D. Siri, D. Gigmes, C. Lefay, Y. Guillaneuf, Angew. Chem. Int. Ed. 2020, 59, 14517-14526.
- [24] R. A. Evans, G. Moad, E. Rizzardo, S. H. Thang, *Macromolecules* 1994, 27, 7935-7937.
- [25] J. M. J. Paulusse, R. J. Amir, R. A. Evans, C. J. Hawker, J. Am. Chem. Soc. 2009, 131, 9805-9812.
- [26] L. P. D. Ratcliffe, C. Couchon, S. P. Armes, J. M. J. Paulusse. Biomacromolecules 2016, 17, 2277-2283.
- [27] J. Du, B. Choi, Y. Liu, A. Feng, S. H. Thang, *Polym. Chem.* 2019, 10, 1291-1298.
- [28] R. A. Smith, G. Fu, O. McAteer, M. Xu, W. R. Gutekunst, J. Am. Chem. Soc. 2019, 141, 1446-1451.
- [29] N. M. Bingham, P. J. Roth, Chem. Commun. 2019, 55, 55-58.
- [30] M. P. Spick, N. M. Bingham, Y. Li, J. de Jesus, C. Costa, M. J. Bailey, P. J. Roth, *Macromolecules* 2020, 53, 539-547.
- [31] H. Huang, B. Sun, Y. Huang, J. Niu, J. Am. Chem. Soc. 2018, 140, 10402-10406.
- [32] B. Quiclet-Sire, S. Z. Zard, J. Am. Chem. Soc. 1996, 118, 1209-1210.
- [33] X.Li, X. Yin, P. Wu, Z. Han, Q. Zhu, Chin. J. Polym. Sci. 1998, 16, 25-31.
- 34] B. P. Fors, C. J. Hawker, Angew. Chem. Int. Ed. 2012, 51, 8850-8853.
- [35] H. Zhou, J. A. Johnson, Angew. Chem. Int. Ed. 2013, 52, 2235-2238.
- [36] A. Anastasaki, V. Nikolaou, Q. Zhang, J. Burns, S. R. Samanta, C. Waldron, A. J. Haddleton, R. McHale, D. Fox, V. Percec, P. Wilson, D. M. Haddleton, *J. Am. Chem. Soc.* 2014, 136, 1141-1149.
  [37] N. J. Treat, H. Sprafke, J. W. Kramer, P. G. Clark, B. E. Barton, J. Read
- [37] N. J. Treat, H. Sprafke, J. W. Kramer, P. G. Clark, B. E. Barton, J. Read de Alaniz, B. P. Fors, C. J. Hawker, J. Am. Chem. Soc. 2014, 136, 16096-16101.
- [38] M. Chen, M. Zhong, J. A. Johnson, Chem. Rev. 2016, 116, 10167-10211.
- [39] J. C. Theriot, C.-H. Lim, H. Yang, M. D. Ryan, C. B. Musgrave, G. M. Miyake, *Science* 2016, 352, 1082-1086.
- [40] E. E. Stache, V. Kottisch, B. P. Fors, J. Am. Chem. Soc. 2020, 142, 4581-4585.
- [41] K. Jiang, S. Han, M. Ma, L. Zhang, Y. Zhao, M. Chen, J. Am. Chem. Soc. 2020, 142, 7108-7115.
- [42] Q. Quan, M. Ma, Z. Wang, Y. Gu, M. Chen, Angew. Chem. Int. Ed. 2021, 60, 2-11.
- [43] A. J. Perkowski, W. You, D. A. Nicewicz, J. Am. Chem. Soc. 2015, 137, 7580-7583
- [44] M. S. Messina, J. C. Axtell, Y. Wang, P. Chong, A. I. Wixtrom, K. O. Kirlikovali, B. M. Upton, B. M. Hunter, O. S. Shafaat, S. I. Khan, J. R. Winkler, H. B. Gray, A. N. Alexandrova, H. D. Maynard, A. M. Spokoyny, J. Am. Chem. Soc. 2016, 138, 6952-6955.
- [45] V. Kottisch, Q. Michaudel, B. P. Fors, J. Am. Chem. Soc. 2016, 138, 15535-15538.
- [46] Q. Michaudel, T. Chauvire, V. Kottisch, M. J. Supej, K. J. Stawiasz, L. Shen, W. R. Zipfel, H. D. Abruna, J. H. Freed, B. P. Fors, J. Am. Chem. Soc. 2017, 139, 15530-15538.
- [47] X. Zhang, Y. Jiang, Q. Ma, S. Hu, S. Liao, J. Am. Chem. Soc. 2021, 143, 6357-6362.
- [48] K. A. Ogawa, A. E. Goetz, A. J. Boydston, J. Am. Chem. Soc. 2015, 137, 1400-1403.
- [49] A. E. Goetz, A. J. Boydston, J. Am. Chem. Soc. 2015, 137, 7572-7575.
- [50] T. Krappitz, K. Jovic, F. Feist, H. Frisch, V. P. Rigoglioso, J. P. Blinco, A. J. Boydston, C. Barner-Kowollik, J. Am. Chem. Soc. 2019, 141, 16605-16609.
- [51] H. Lai, J. Zhang, F. Xing, P. Xiao, Chem. Soc. Rev. 2020, 49, 1867-1886.
- [52] J. Xu, K. Jung, A. Atme, S. Shanmugam, C. Boyer, J. Am. Chem. Soc. 2014, 136, 5508-5519.
- [53] J. Xu, K. Jung, N. A. Corrigan, C. Boyer, Chem. Sci. 2014, 5, 3568-3575.
- [54] J. Xu, S. Shanmugam, H. T. Duong, C. Boyer, *Polym. Chem.* 2015, 6, 5615-5624.
- [55] S. Shanmugam, J. Xu, C. Boyer, *J. Am. Chem. Soc.* **2015**, *137*, 9174-9185.
- [56] N. Corrigan, S. Shanmugam, J. Xu, C. Boyer, Chem. Soc. Rev. 2016, 45, 6165-6212.
- [57] J. Yuan, W. Wang, Z. Zhou, J. Niu, *Macromolecules* **2020**, *53*, 5655-5673.
- [58] G. I. Peterson, T.-L. Choi, *Chem. Sci.* **2020**, *11*, 4843-4854.
- [59] N. Li, D. Ding, X. Pan, Z. Zhang, J. Zhu, C. Boyer, X. Zhu, *Polym. Chem.* 2017, 8, 6024-6027.
- [60] H. Huang, W. Wang, Z. Zhou, B. Sun, M. An, F. Haeffner, J. Niu, J. Am. Chem. Soc. 2019, 141, 12493-12497.
- [61] N. A. Lynd, R. C. Ferrier, B. S. Beckingham, *Macromolecules* **2019**, 52, 2277-2285.
   [62] B. S. Beckingham, G. E. Sanoja, N. A. Lynd, *Macromolecules* **2015**, 48,
- 6922-6930.

  [63] D. Neugebauer, K. Matyjaszewski, *Macromolecules* **2003**, 36, 2598-
- 2603. [64] K. O'Leary, D. R. Paul, *Polymer* **2004**, *45*, 6575-6585.
- [65] Z. Florjanczyk, *Prog. Polym. Sci.* **1991**, *16*, 509-560.
- [66] G. Qiu, K. Zhou, L. Gao, J. Wu, *Org. Chem. Front.* **2018**, *5*, 691-705.

- [67] K. Hofman, N.-W. Liu, G. Manolikakes, *Chem. Eur. J.* **2018**, *24*, 11852-11863.
  [68] A. V. Marenich, C. J. Cramer, D. G. Truhlar, *J. Phys. Chem. B* **2009**, *113*, 6378-6396.
  [69] J. S. Hwang, C. P. Tsonis, *J. Polym. Sci., Part A: Polym. Chem.* **1993**, 31, 1417-1421.



# **Entry for the Table of Contents**



A general approach to degradable vinyl random copolymers via photocontrolled radical ring-opening cascade copolymerization (rROCCP) is developed. A variety of acrylates or acrylamides can be copolymerized with the macrocyclic allylic sulfone with near-unity comonomer reactivity ratios at all feed compositions. The unusual reversible inhibition of chain propagation by sulfur dioxide in rROCCP was resolved by reducing the solubility of sulfur dioxide.

